# The straddle carrier as an example for the electrification of mobile machines

Dr. Armin U. Schmiegel, REFU Drive GmbH, University of Applied Science, Reutlingen

## 1. Introduction

Climate change and rising energy prices, as well as the continuous improvement of power electronic components, storage and drive technology, are driving the shift towards the electrification of mobile machines [1], [2], [3]. The design of a mobile machine proves to be a complex task. For example, the various requirements for power consumption and output and the requirements for torque and speed must be considered. In addition, the number of possibilities for realisation is very large. This starts with the choice of drive technology, diesel-electric, hybrid or all-electric, and then goes on to the choice of components for the design of motor and transmission.

Already in [4] we presented a method that allows a quick preselection without any results. In this report, we want to apply this approach to the design of a straddle carrier. The core element is the system description via power flows. With the help of an analysis of the power flows, we are able to design a diesel-electric, an all-electric and a hybrid powertrain and compare them with each other. In doing so, we take advantage of the fact that a device-independent formulation is possible with the help of the power flow analysis, for which individual optimisations are then carried out.

## 2. Straddle Carrier

In Figure 2-1 shows a straddle carrier. This is a container crane travelling on stilts that can stack up to three containers, depending on the configuration. Also shown in Figure 2-1 also shows the components for a hybrid drive train. The vehicle uses four electric travel drives and an electric drive for the hoist. These components are connected to the energy sources via a high-voltage intermediate circuit. Since a hybrid powertrain contains both a diesel unit and a battery, the design of a diesel-electric or an all-electric powertrain is thus also included in the illustration.

The diesel-electric drive train consists of a combustion engine, a generator and a rectifier. The rectifier can be passive or active. In the case of a passive rectifier, rectification takes place via a diode bridge. With an active rectifier, the alternating current of the generator is actively rectified by an inverter. This has the advantage that the voltage level on the connecting DC link is kept constant and does not depend on the speed of the combustion engine. The DC link voltage thus becomes significantly more stable.

The battery is shown in Figure 2-1 is connected directly to the DC link. Alternatively, the use of a DC/DC converter would be conceivable. Due to the size of the battery and the required charging and discharging power, the DC/DC controller is not used in this consideration. However, this means that all other power electronic components, inverters and rectifiers must adapt to the voltage curve of the battery. This may have an influence on the dynamic behaviour of the drives.[5]

Four drive motors and a hoist are connected to the battery or generator as consumers. They draw their energy via the DC link. To simplify matters, an analysis of the auxiliary drives, air conditioning in the driver's cab, the hydraulic pump and the 24-volt on-board power supply is omitted here. For a complete design, these systems must of course also be considered.

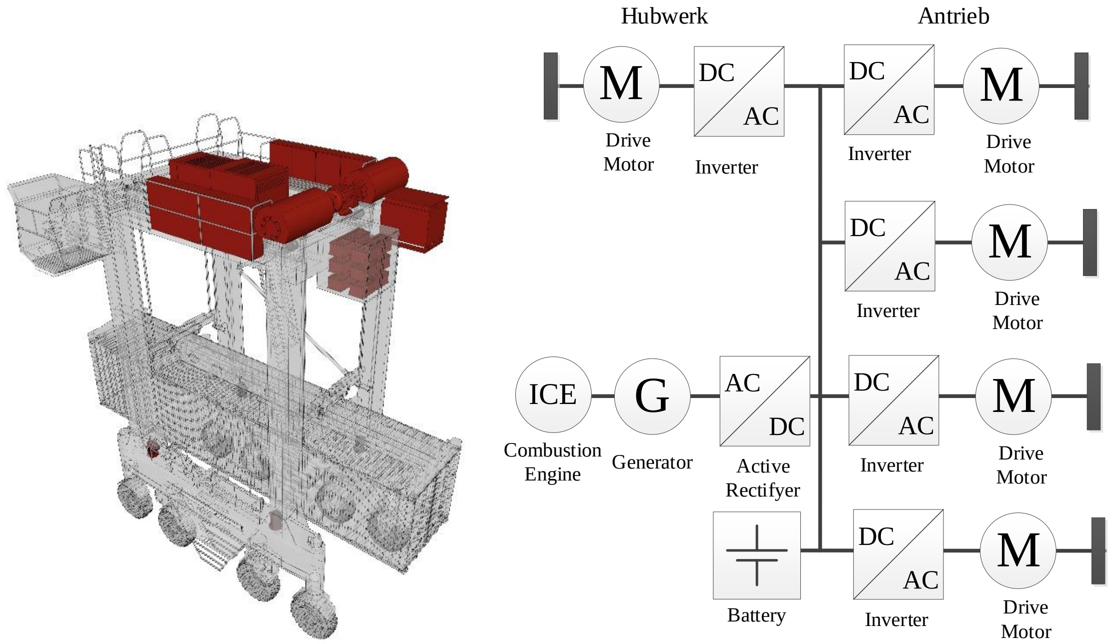


*Figure 2-1 : Illustration of a hybrid powered straddle carrier (left) and its electrical components (right).*

For electrification, the question is which approach is most suitable to realise the requirements and the target costs. For this, however, an optimal configuration must be determined for each approach. With the analysis of the power flow diagram[6]-[9] a simple tool is available that can carry out these analyses for different realisations. The approach and the necessary individual steps are described below.

## 3. Description of the straddle carrier using the power flow diagram

The power flow diagram describes energy systems in an abstract way. [6]-[9] The basic idea here is that the overall system is divided into power sources, storage and consumers, between which power transport takes place. In the case of the hybrid straddle carrier, the diesel generator set was interpreted as a power source, the battery as storage, and the hoist and drives as consumers. To reduce complexity, the four drive motors are combined into one consumption node.

In Figure 3-1 shows the power flow diagram for the straddle carrier. $H$ is the node for the hoist, $S$ the node for the battery, $A$ the node for the drive and $G$ stands for the generator. The nodes alone are of no use. This only arises by describing which power flows are permitted. A power flow from the node $A$ to $B$ is denoted with $A_B$ is used. The transport losses are described by the power-dependent efficiency $\eta_{AB}(A_B)$ described.

In the case of a hybrid driveline, the power from the generator can be transported to the hoist, the storage and the drive. This is determined by the power flows $G_H, G_S$ and $G_A$ described. The accumulator can transport its power to the hoist $S_H$ and to the drive $S_A$ but can also draw power from both motors through recuperation. $A_S, H_S$. Furthermore, and this is a special feature of storage nodes, it can draw power from the past or shift power into the future. $S_S(\pm\Delta)$.

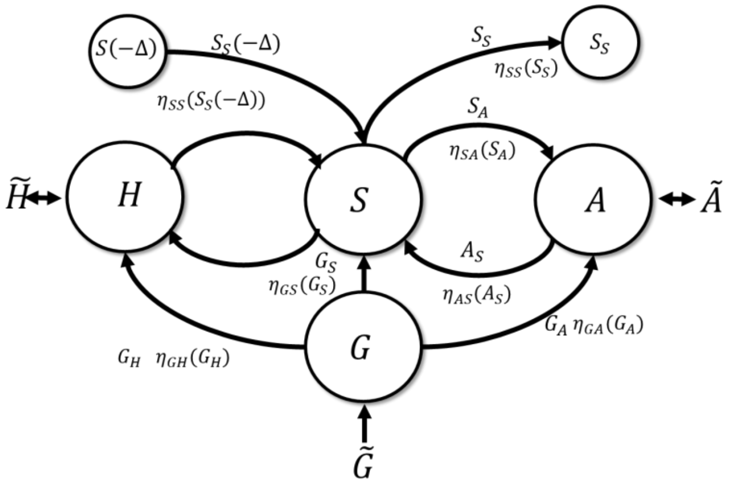


*Figure 3-1 : Power flow diagram of a straddle carrier with a hybrid drive train. The straddle carrier is described using four power nodes.* H *for the hoist,* A *for the drive,* S *for the storage and* G *for the generator.*

The following equations summarise the relationships between the power flows:

$$\tilde{G} = G_S + G_A + G_H$$

$$0 = \eta_{GS}G_S + \eta_{AS}A_S + \eta_{HS}H_S + \eta_{SS}S_{S(-\Delta)} - (S_A + S_H + S_S)$$

$$\tilde{A} = \eta_{SA}S_A + \eta_{GA}G_A - A_S$$

$$\tilde{H} = \eta_{SH}S_H + \eta_{GH}G_H - H_S$$

$\tilde{G}$ is the consumption profile of the generator and represents a balance sheet variable. $\tilde{A}$ and $\tilde{H}$ are the load profiles of the hoist and the traction drive, respectively. These load profiles must be specified in order to determine the load flows in the overall system.

For the design of the drive train, the question arises as to what maximum power is required. In the load flow diagram, this question is described by the permitted value ranges of the power flows and additional constraints:

$$G_S + G_A + G_H \leq G_{\text{max}}$$

$$H_S + A_S + G_S \leq S_{\text{charge}}$$

$$S_H + G_H \leq H_{\text{max}}$$

$$S_A + G_A \leq A_{\text{max}}$$

The first equation states that the sum of the power flows from the generator to the other nodes must not be greater than the total power of the generator. The second equation makes a similar statement for the accumulator only and the last two equations restrict the power flows from the hoist and the drive train.

The aim of the regulation is to minimise losses:

$$\min Y = \Big(\big(G_S(1-\eta_{GS}) + A_S(1-\eta_{AS}) + H_S(1-\eta_{HS}) + S_S(-\Delta)(1-\eta_{SS}) + S_A(1-\eta_{SA}) + G_A(1-\eta_{GA}) + S_H(1-\eta_{SH}) + G_H(1-\eta_{GH})\big)\Big)$$

Thus, the task for the system design is relatively simple: The load profile is run for each system configuration. At each point in time, the power must be distributed between the nodes in such a way that the loads are supplied and the boundary conditions are met. We can now formulate a strategy for each system according to which this has to be done. However, there is then the risk that we let hidden assumptions about the system behaviour flow into the control, which falsify the result. For this reason, it makes more sense to solve the optimisation task. In this way, the mathematically optimal power flow is selected in each case. Each subsequent realisation must then measure itself against this optimal solution.

## 4. Power flow of a hybrid straddle carrier

In Figure 4-1 shows the load profile of a straddle carrier. [10], [11]. It is noticeable that the dynamics and also the power demand for the drives are very high. The observed load jumps take place on a time scale of tenths of seconds and can vary from $350\ \mathrm{kW}$ to $-250\ \mathrm{kW}$ jumps.

The hoist has a slightly lower dynamic, but here too we see load jumps that can be observed on a time scale of tenths of a second.

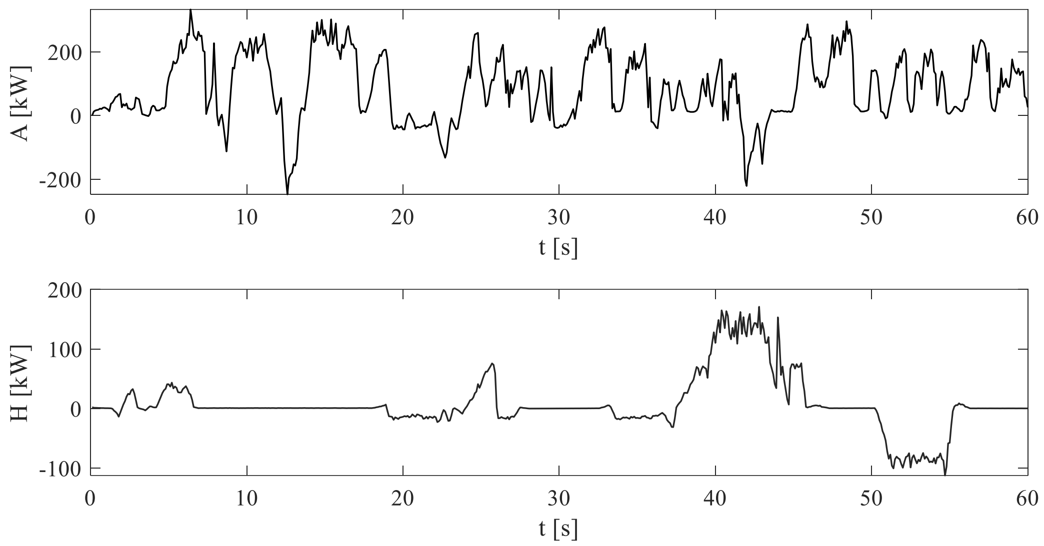


*Figure 4-1 : Load profile of a straddle carrier* [10]

In addition to the load profile, the efficiencies of the power transmission must be defined. In Figure 4-2 these are shown. The efficiency is seen here as a function of the power. It results from a consideration of the constant, linear and quadratic losses[6], [7]. The constant losses dominate the low power range, while the quadratic components dominate at high powers. To simplify, we have assumed that $\eta_{SA} = \eta_{AS}$ and $\eta_{SH} = \eta_{HS}$ is.

In these studies, we assume a maximum efficiency of the generator of approx. 40%. This includes the efficiency of the combustion engine and the electric machine. The influence of the power electronics is only slightly noticeable here. The battery in combination with the power electronics, on the other hand, has an efficiency range of 80% to 96%. It is therefore obvious that the storage unit is always the preferred solution in this application.

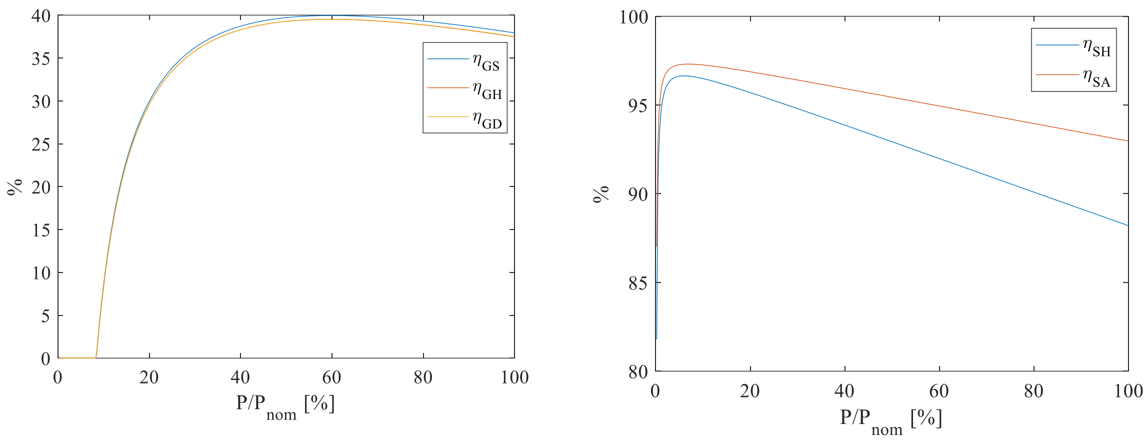


*Figure 4-2 : Efficiencies of power flows used.*

Now let's look at the figure shown in Figure 4-3 of the power flow of the different components. It can be seen that in this configuration there is a situation with the drive where the components cannot serve the power. For the configuration of the system, this means that the design must be adjusted or this peak is accepted. Furthermore, it is noticeable that $G_A + S_A$ is always greater than the demanded power. This particularly affects those areas where the generator is active. Here the low efficiency of the generator becomes visible. Because with the load there is not $G_A$ but $G_A \cdot \eta_{GA}(G_A)$ arrives. The operation management must take these transmission losses into account and provide suitable excess capacity.

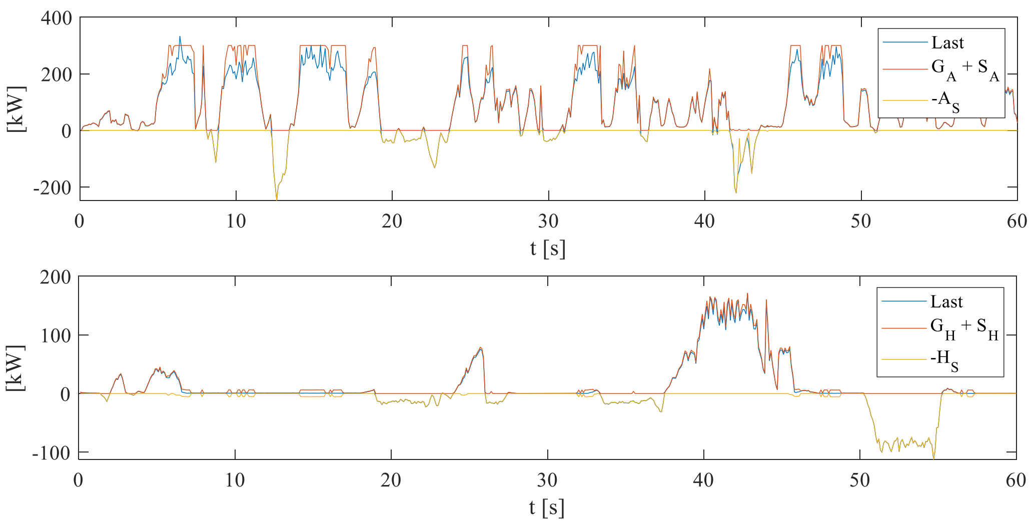


*Figure 4-3 : Power flows for the services described in Figure 4-1 shown in Figure 41.*

## 5. Power and energy demand

In this section, the various drive trains are to be optimally configured and the data compared with each other. In doing so, we consider an operation of $360$ s.

### 5.1 Diesel-electric Straddle Carrier

We begin with the consideration of the pure diesel-electric vehicle. In this case, the storage node is omitted $S$ and all power flows leading to or away from this node. The system of equations is simplified accordingly. The design task is now to select the power class for the diesel generator that has the lowest losses and also covers the power demand. The efficiency curve of the generator is scaled in relation to the nominal power. The maximum efficiency is always at $60\%$ $P_{\max}$ with an efficiency of $40\%$ and decreases to $38\%$ at $P_{\max}$ downwards. Loads below $8\%$ $P_{\max}$ cannot be served, as here the efficiency drops to zero.

In Figure 0-1 shows the portion of the load that can no longer be supplied at a given generator output. At low generator output, the demand can only be partially served. If the power increases, this proportion of unserved loads is reduced linearly. From approx. $300$ kW the proportion is reduced considerably, because the now missing load peaks occur much less frequently. From a generator output of $450$ kW the generator can cover the load completely.

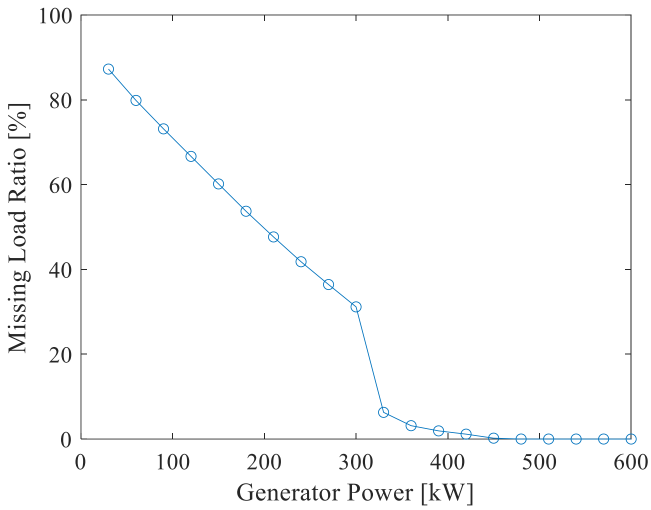


*Figure 0-1 : Proportion of load not supplied as a function of generator output.*

However, it is not sufficient to look at the load cover alone to determine the optimal generator output. If we were to do this, the optimal power would be between $310$ kW and $450$ kWdepending on how important the benefit of full load coverage is. For the design, we also need to look at efficiency and energy consumption. Since we have defined the maximum efficiency of the generator to always be 60% of the maximum power, it may well be that a different configuration makes more sense because it has a higher overall efficiency and moderate consumption. In Figure 0-2 therefore shows the overall efficiency of the experiment as well as the consumption.

As we can see, the efficiency increases to $300$ kW increases. Here we can see very nicely the effect that at higher powers the efficiency of the generator is also higher in total. From $300$ kW the efficiency drops. Here, the generator is designed in such a way that it also covers rare events well.

can. However, this has the consequence that most of the load coverage takes place in the light load range. From Figure 4-2 it is known, however, that the efficiency is significantly lower in the low-load range, since the constant losses dominate the efficiency here.

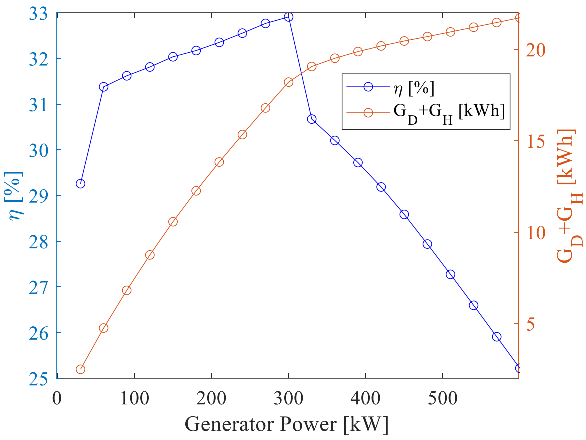


*Figure 0-2 : Total efficiency over* $360\ \mathrm{s}$ *and the amount of primary energy consumed.*

As you can see, consumption is also increasing. By $300\ \mathrm{kW}$ this is essentially because more energy is also used for propulsion. From $300\ \mathrm{kW}$ the effect of decreasing efficiency dominates. This can be seen from the different slope of the sales curve $(G_D + G_H)$ can be seen.

The optimum design point for the generator from an energy point of view is the generator output at which these effects merge. This would $300\ \mathrm{kW}$ would indeed be the case. However, this means that the straddle carrier cannot run some load points, as can be seen in Figure 0-3 can be seen. Here it must be weighed up whether these performance losses, which occur ten times within 6 minutes, can be justified or whether the higher energy demand must be accepted.

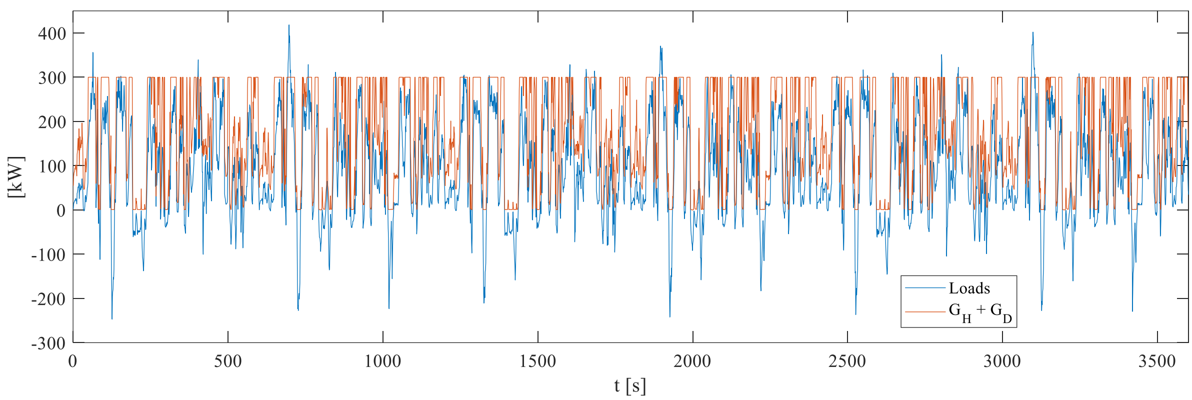


*Figure 0-3 : Load coverage and primary energy consumption for a generator-driven straddle carrier at the energetically optimal operating point.*

## 5.2 Fully electric straddle carrier

In the all-electric case, no generator is used. The battery alone is used here to supply the vehicle. This means that the power paths $G_D, G_H$ and $G_S$ are not used. Since we are considering a period of only 3 minutes, we can assume the storage capacity to be sufficiently large, i.e. the power flow $S_S(\pm\Delta)$ is of secondary importance.

In electrochemical storage, the charge rate is usually different from the discharge rate. For lithium-ion batteries that use lithium iron phosphate as the cathode material, discharge rates of 2-4C are possible, while charge rates often remain limited to 1C. To account for this effect, we assume that the charge rate is half the discharge rate.

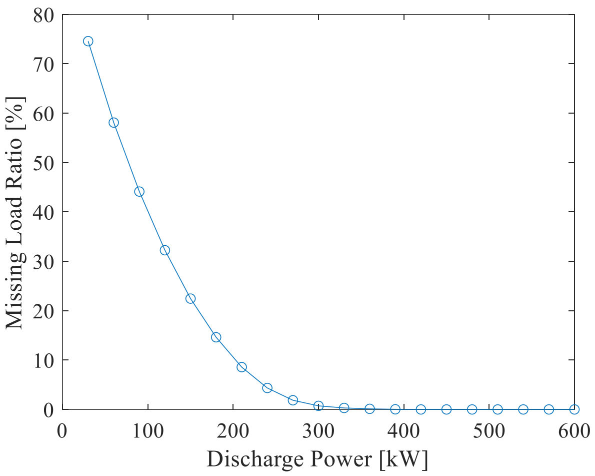


*Figure 0-1 : Proportion of unsupplied load as a function of discharge power.*

Since the same load profile is used as for a diesel-electric straddle carrier, the proportion of unsupplied power will behave similarly. This is shown in Figure 0-1 can also be seen. However, this curve is much steadier than for a diesel-electric system. It can also be seen that less discharge power is needed to ensure a higher coverage. With a generator output of 300 kW the proportion of unsupplied load was still at 0,5%. With an all-electric straddle carrier, this proportion is smaller. This is due to the high efficiency of the system. As we can see in Figure 0-2 we can see that the overall efficiency is already at 200 kW at 94%whereas with a diesel-electric system the efficiency was at 32% for a diesel-electric system. Here, in addition to the efficiency of the components, there is also the recuperation as a supporting effect.

Unlike the diesel-electric vehicle, efficiency and overall consumption stabilise for higher discharge rates. While the overall efficiency already improves at 150 kW with 94% this is only the case for consumption from 300 kW with 10 kWh can be observed. This corresponds to half the consumption of the diesel-electric vehicle.

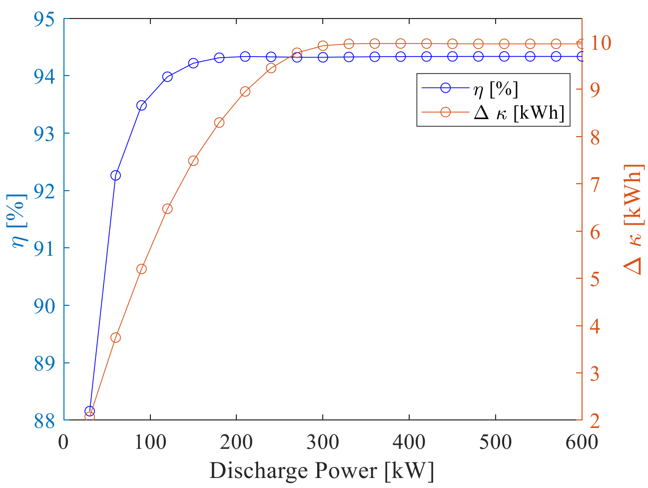


*Figure 0-2 : Total efficiency and utilised storage capacity for your all-electric straddle carrier at different discharge rates.*

## 5.3 Diesel-hybrid powered straddle carrier

The last system configuration to be considered here is the diesel-hybrid powered straddle carrier (Figure 2-1). Here the system shown in Figure 3-1 is used in its entirety.

In our consideration, we want to look at the already described variables as a function of the generator power and the discharge power. As we have already seen from the previous investigations, a power of approx. $300\ \mathrm{kW}$is sufficient to cover the power demand of the application. Above $300\ \mathrm{kW}$ only individual demand peaks have to be supplied. Due to the lower efficiency of the generator, the loss fraction at $300\ \mathrm{kW}$ of the diesel-electric straddle carrier is significantly higher than that of the all-electric straddle carrier.

In the hybrid straddle carrier we see a mixture of both behaviours. In Figure 0-3 the missing load ratio is shown as a function of the generator power and the discharge power of the battery. At a low discharge power of the battery, the behaviour of the generator clearly dominates. The missing load ratio is clearly increased, but decreases with the generator power. As the discharge power of the battery increases, the missing load ratio decreases very quickly. This is due to the high efficiency of the transmission paths from the battery to the consumers. From a final charging power of $200\ \mathrm{kW}$ and a generator output of $100\ \mathrm{kW}$ the missing load ratio is negligible. This is where the fact that the generator can now work at its optimum operating point comes into play, i.e. its losses are minimised while the more efficient battery covers the remaining demand.

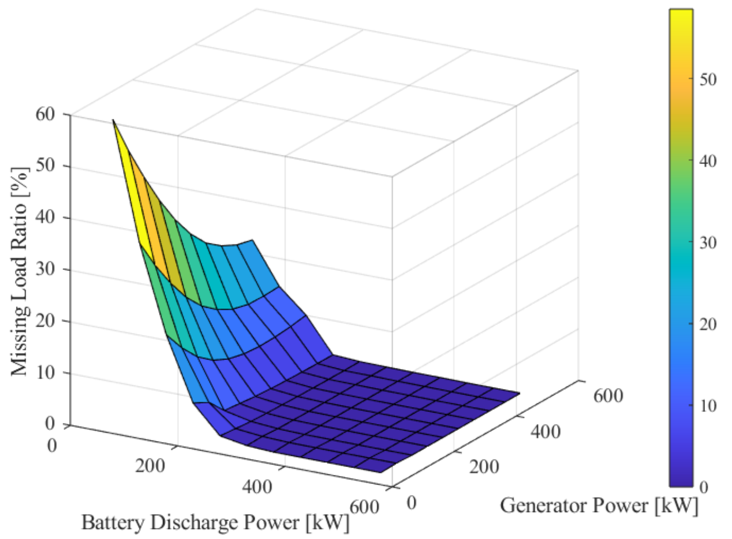


*Figure 0-3 : Missing Load Ratio of a hybrid-powered straddle carrier as a function of generator power and battery discharge power.*

Unfortunately, the advantage of the distributed load is not reflected in the energy consumption of the hybrid solution (Figure 0-4). The all-electric straddle carrier always has a significantly lower energy consumption than the diesel-electric straddle carrier. A mixture of the two sources therefore only ensures that the total energy consumption increases. However, this does not necessarily argue against a diesel-electric straddle carrier. For the six-minute load profile studied here, the all-electric straddle carrier requires $10\ \mathrm{kWh}$which corresponds to a consumption of $800\ \mathrm{kWh}$ for an 8-hour shift. If we set the battery to $200\ \mathrm{kWh}$ discharge capacity, the storage capacity is reduced to $8\ \mathrm{kWh}$which corresponds to a shift demand of 640 kWh. At a battery system price of 150€/kWh, this corresponds to a cost advantage of 24,000€. The missing power is compensated by a generator, which has an energy demand of $7\ \mathrm{kWh}$ per six minutes, i.e. $560\ \mathrm{kWh}$ per shift. This corresponds to approx. 56l of fuel and thus costs of approx. 112€ (at 2€/l).

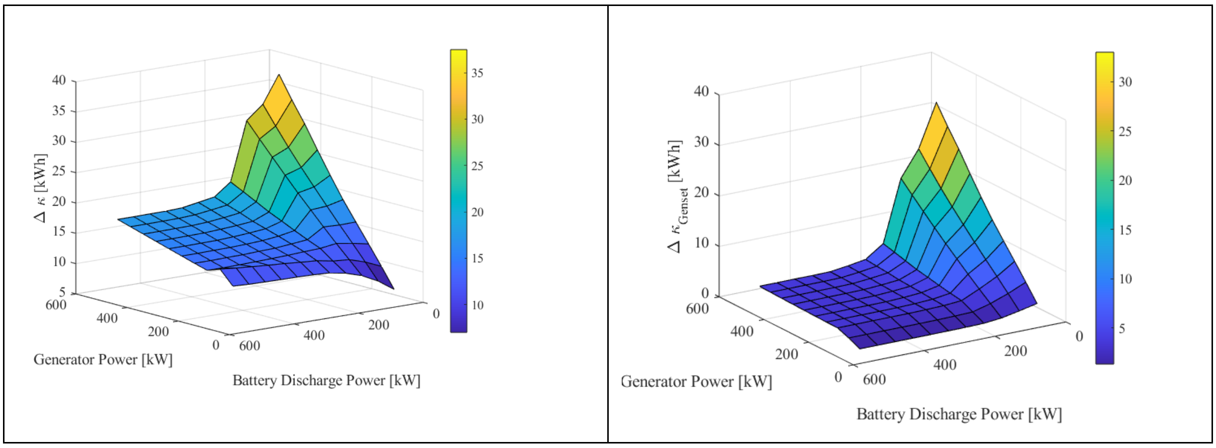


*Figure 0-4 : Energy consumption of a hybrid operated straddle carrier.*

We also expect a mixture of the two individual experiments in terms of efficiency. As shown in Figure 0-5 it can be seen that at low generator power the battery dominates high efficiency. This is proportionally reduced by the generator efficiency. Dis discussed combination of a generator with 100 kW power and a battery with 200 kW discharge power also proves to be a sensible combination here.

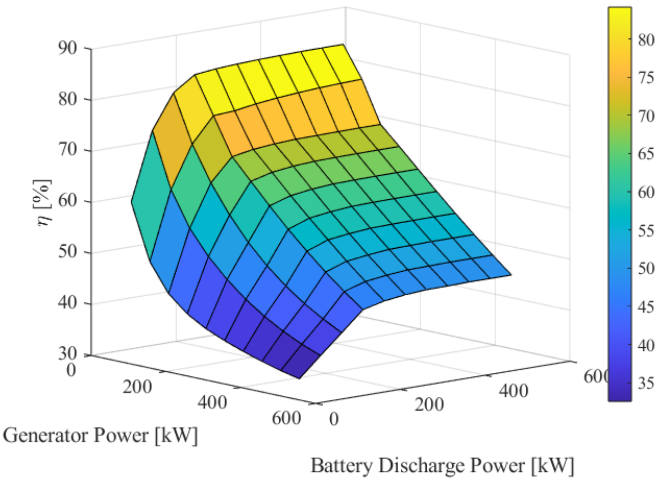


*Figure 0-5 : Efficiency of the hybrid straddle carrier as a function of generator power and battery discharge power.*

## 6. Conclusion

With the help of the power flow diagram, we were able to determine optimal system configurations for three different drive trains. This information can now be integrated into a preliminary economic analysis in which manufacturing and operating costs as well as expected yields are offset against each other.[6], [7]

In our example, the required peak power was given by the load profile. Here, a static analysis of the histogram would already have sufficed information about the load demand. However, the analysis provides us with statements about the influence of recuperation and consumption and takes into account the losses of individual transmission paths.

Due to the formulation as a non-linear optimisation problem, the results do not contain any assumptions about the operational management. The results given here are to be regarded as optimal results of a certain realisation. This has the advantage that a baseline is always already available for orientation when developing an operation management.[9], [12], [13]. However, no forecast of the load curve was integrated in the analysis carried out here. An extended formulation of the optimisation task over the entire period would make it possible to identify the globally optimal operation management. Due to the high dynamics reflected in the load profile, this is associated with a high computational time expenditure. However, it could be shown in other systems that the knowledge gained from this indicates what optimal operation management would have to look like.[13]

The analysis presented here considered only one power electronic realisation of the drive train from Figure 2-1. If, in addition to the question of whether a diesel-electric, hybrid or all-electric powertrain is to be realised, there is also the question of the choice of components, the analysis is extended by considering different efficiencies. $\eta_{AB,i}(A_B)$where $i$ corresponds to a component selection. This component selection must then be expanded to include the performance specifications. $A_B \in \{0, A_B^{\mathrm{max,i}}\}$ to be added.

The power flow diagram enables us to easily determine the optimal system configurations and thus represents a first step for a quantitative system design. It allows us to look at different issues in parallel and thus only start with labour-intensive detailed analyses at a significantly later stage. This allows a sensible pre-selection when electrifying mobile machines that have a large number of actuators integrated.

## References

[1] A. Lajunen, P. Sainio, L. Laurila, J. Pippuri-Mäkeläinen, and K. Tammi, "Overview of powertrain electrification and future scenarios for non-road mobile machinery," *Energies (Basel)*, vol. 11, no. 5, 2018, doi: 10.3390/en11051184.

[2] M. Liukkonen, A. Lajunen, and J. Suomela, "Feasibility study of fuel cell-hybrid powertrains in non-road mobile machineries," *Autom Constr*, vol. 35, pp. 296-305, 2013, doi: 10.1016/j.autcon.2013.05.019.

[3] K. Tammi, P. Sainio, and D. Student, "Hybrid and electric Non-Road Mobile Machines ( NRMM ) For further interest on NRMM roadmap," 2017.

[4] Armin U. Schmiegel, "From the smoking exhaust to the clean socket Design steps from the diesel-powered mobile machine to the all-electric mobile machine Part 1 - Power and Energyconsiderations," Reutlingen, 2022.

[5] Armin U. Schmiegel, "From the smoking exhaust to the clean socket Design steps from the diesel-powered mobile machine to the all-electric mobile machine Part 2 - The triad of battery, inverter and motorMotor," Reutlingen, 2022.

[6] A. U. Schmiegel, *Energy Storage Systems,* vol. in Press. Oxfort: Oxford University Press, 2022.

[7] A. U. Schmiegel, *Energiespeicher für die Energiewende*. Munich: Hanserverlag, 2019.

[8] A. U. Schmiegel and A. Kleine, "Upper economical performance limits for pv storage systems," in *28th European Photovoltaic Solar Energy Conference*, 2013, pp. 1-20.

[9] S. Ried, A. U. Schmiegel, and N. Munzke, *Efficient Operation of Modular Grid-Connected Battery Inverters for RES Integration*. 2020. doi: 10.1007/978-3-030-32157-4_10.

[10] J. Kukkaro, "Straddle Carrier Electric Powertrain Optimization," no. August, 2016.

[11] P. Hangga and T. SHINODA, "Study on Efficiency Measurement Technique for Container Handling Equipment - Application to Hybrid Straddle Carrier," no. JULY 2014, 2014.

[12] A. U. Schmiegel, "Residential PV Storage Systems - storage size matters - Residential PV Storage Systems," in *Intersolar Conference,* 2013.

[13] A. Kleine and A. U. Schmiegel, "Optimized Operation strategies for PV Storages systems - Yield limitations, optimized battery configuration and the benefit of a perfect forecast," *Energy Procedia*, vol. 46, pp. 104-113, 2014, [Online]. Available: http://dx.doi.org/10.1016/j.egypro.2014.01.163